Published in final edited form as:
Magn Reson Med. 2009 May ; 61(5): 1090–1095. doi:10.1002/mrm.21914.

Improved half RF slice selectivity in presence of eddy currents with out-of-slice saturation

Sonal Josan[1,2], **Elena Kaye**[1,2], **John M. Pauly**[1], **Bruce L. Daniel**[2], and **Kim Butts Pauly**[2]
[1]Department of Electrical Engineering, Stanford University

[2]Department of Radiology, Stanford University

Abstract

Ultrashort echo time imaging with half RF pulse excitation is sensitive to eddy currents induced by the slice-select gradient that distort the half pulse slice profile. This work demonstrates improvements to the half pulse profile by using spatial saturation on both sides of the imaged slice to suppress the out-of-slice magnetization. This effectively improves the selectivity of the half pulse excitation profile. A quadratic phase RF pulse with high bandwidth and selectivity is used to achieve a wide saturation band with sharp edges. Experimental results demonstrate substantially improved slice selectivity and R2* quantitation accuracy obtained with the out-of-slice saturation. This approach is effective in making short T2 imaging and quantitation with half pulses less sensitive to eddy currents.

Keywords

ultrashort echo time; half RF; outer volume suppression; quadratic phase RF

Introduction

Ultrashort echo time (UTE) imaging allows detection of tissues with T2 relaxation times in the sub-millisecond range. Some of the applications for UTE imaging of short T2 species include the musculoskeletal system, lung, plaque, and frozen tissue during cryoablation [1–14]. Conventional imaging methods typically have a minimum echo time (TE) of 1–2 ms, and so are unable to detect these tissues. The minimum echo time in UTE imaging is limited only by the hardware transmit/receive switching times, which are generally about 100 μs, but can be as short as 8 μs [15]. These UTE techniques make it possible to directly image the short T2 tissues. However, robust quantitative assessment of short T2 components *in vivo* remains challenging.

Slice-selective UTE imaging generally uses a half-sinc RF excitation pulse with 2D radial sampling [1]. Slice selection is achieved by adding together the acquisitions from two excitations with the slice-select gradient inverted. However, the half RF excitation pulse is very sensitive to gradient imperfections such as eddy current distortions that cause errors in the slice profile. Several techniques based on accurate characterization of gradients and k-space trajectories have been proposed to compensate for these eddy current distortions [16–20]. Although these corrections have been critical to improve the slice profile for accurate T2* measurement and quantitation, they are time-consuming, and can be difficult to implement.

Correspondence: Sonal Josan, Lucas MRI Center, MC 5488, 1201 Welch Rd., Stanford, CA 94305, Email : sjosan@stanford.edu, Phone : 650-724-8029, Fax : 650-723-5795.

The purpose of this work was to develop a simple and robust method that makes short T2 imaging and quantitation with half pulses less sensitive to eddy currents. Each half pulse excitation individually is not very selective, and excites signal far from the intended slice location. In the ideal case, the slice from each excitation has opposite phase and cancels perfectly to form the desired slice selection. Eddy currents distort the phase and slice profile of each half pulse excitation. Thus, the magnetization from out of the slice does not cancel appropriately when the two excitations are combined, resulting in a distorted slice profile that is not very selective. In this work, spatial saturation is done symmetrically on both sides of the imaging slice to suppress the out-of-slice magnetization. This is done so that imperfect cancellation of magnetization outside the slice does not contaminate the signal. This effectively improves the selectivity of the half pulse excitation profile in a simple and robust way.

This approach is similar to outer volume suppression, generally used in applications such as reduced field-of-view imaging and volume localization in spectroscopy [21–23]. It allows the ability to accurately isolate a region of interest, with minimal signal contamination from the surrounding tissue. This is typically accomplished by using saturation pulses to selectively excite and then dephase the undesired volume magnetization before the imaging sequence. To suppress out-of-slice (or outer-volume) magnetization, a wide saturation band with a sharp profile is needed, which in turn requires an RF pulse with high bandwidth and selectivity. The peak B_1 amplitude of linear phase RF pulses increases with bandwidth. Therefore the B_1 amplitude and power limitations of the RF amplifier and transmit coil restrict the bandwidth achievable with linear phase pulses. Quadratic Phase (QP) RF pulses distribute the RF energy more evenly over the pulse duration compared to linear phase pulses. Thus they can achieve higher excitation bandwidth and improved selectivity (shorter transition widths), for a given maximum B_1 amplitude and pulse duration [24–27]. QP pulses generally have limited use for excitation as the quadratic phase they introduce into the frequency response (*i.e.* slice profile) cannot be refocused by linear gradients. However, saturation pulses do not require a linear phase and benefit from having nonlinear phase dispersion of the saturated magnetization. Hence, a quadratic phase RF pulse was used for spatial saturation in this work.

Method

Quadratic Phase RF pulse design

The Shinnar-Le Roux (SLR) transform [28] describes an RF pulse with two complex polynomials A(z) and B(z), which represent FIR filters. In this work, we use the approach described by Schulte *et al* [25], where the B polynomial is designed using the complex Remez exchange algorithm to have a quadratic phase and equi-ripple filter coefficients. The corresponding minimum phase A polynomial is generated through the Hilbert transform. The SLR transform is used to convert the polynomials into an RF pulse. When the phase of A is negligible, the phase of the RF will be similar to that of the B polynomial, thus obtaining an RF pulse with quadratic phase modulation.

Increasing the amount of quadratic phase of the RF pulse distributes the RF energy more evenly over the pulse duration, thus reducing the peak B_1. However, increasing values of quadratic phase also lead to greater error in the pulse profile. To achieve the desired out-of-slice suppression for this work, a large bandwidth and a small transition width was required to achieve a wide saturation band with very sharp edges. A QP RF pulse was designed with flip angle of 90°, time-bandwidth product (TBW) = 34, pulse duration = 8 ms, bandwidth (BW) = 4.25 kHz, fractional transition width = 0.15, B_{1max} = 0.079 G, and ripple amplitude ≤2%, to achieve a saturation band 4.5 cm wide with transition width of 2 mm. This QP RF pulse was then cosine modulated to obtain two saturation bands on each side of the slice to

be imaged. The gap between the edges of the saturation bands was 1 cm. After cosine modulation, the peak amplitude of the pulse was B_1 = 0.158 G (to achieve the same flip angle), which was close to the limit of the amplifier. This pulse and its slice profile, as shown in Fig. 1, was used in all experiments in this work.

Experiments

All experiments were performed on a 0.5T GE Signa SP interventional MR scanner (maximum gradient amplitude = 1.2 G/cm, maximum slew rate = 1.6 G/cm/ms). The excitation part of the 2D UTE imaging sequence used is shown in Fig. 1a. The QP saturation RF pulse along with a dephasing gradient is played out before the half pulse excitation. Two excitations with inverted slice-select gradients, shown by the dotted line in the figure, are combined to form the final slice. A radial readout with ramp sampling is used, and this sequence is repeated every TR. The QP saturation RF pulse was phase-cycled to effectively spoil the transverse magnetization [29]. The UTE pulse sequence achieved a minimum TE of 100 μs for the transmit/receive birdcage coils, and 200 μs for the receive-only surface coils. The echo time TE is defined here as the interval between the end of the half RF and beginning of data acquisition. No extra eddy current compensation beyond that performed routinely on the scanner was done in these experiments.

The QP RF pulse designed here was compared to the default cosine-modulated linear phase saturation pulse available on the scanner. Their suppression profiles were imaged in a phantom, with the saturation bands in the frequency encode direction. The slice-select gradient amplitudes were scaled according to pulse bandwidth to excite the same saturation band thickness. For this experiment, the gap between the saturation bands was 2 cm. A half pulse excitation with TE = 100 μs was used. The QP pulse achieved a BW = 4.25 kHz compared to the linear phase pulse BW = 1 kHz. Both saturation pulses had the same time duration of 8 ms. Peak B1 of the linear phase pulse was 0.11 G, compared to 0.158 G for the QP pulse.

Several phantom experiments were performed to demonstrate the improved slice selectivity obtained with out-of-slice saturation. The slice profile of the half pulse, with and without the QP saturation pulse, was imaged in a doped water cylindrical phantom with a long T2 (~100 ms). The slice profile was measured by placing the readout in the slice select direction.

In other experiments, several short T2 phantoms were imaged with a long T2 phantom placed adjacent to it in the slice select direction. The phantom setup was such that the slice to be imaged had short T2 vials in it, with long T2 signal close to, but outside, the slice (~1–2 cm away). Images were acquired at four different echo times (TE = 0.1/0.4/0.7/1 ms for Fig. 4 and TE = 0.2/0.5/0.8/1.1 ms for Fig. 5) with the half pulse excitation, with and without the saturation pulse. A repetition time TR = 35 ms was used for all acquisitions. R2* maps were calculated by exponentially fitting the signal at different TEs on a pixel-by-pixel basis.

The T2* values in the phantoms were calculated by imaging the phantoms separately with non-slice-selective excitation, in order to avoid eddy current errors. The values were found to be in the range of 0.4 – 20ms. T2* values were converted to R2* values and compared to show the improvement in quantitation obtained by improved slice selection through the use of the QP saturation pulses.

The effectiveness of the saturation pulse in removing out-of-slice signal contamination is also illustrated in an *ex vivo* tissue freezing experiment, and an *in vivo* canine prostate cryoablation experiment. An *ex vivo* tissue sample was frozen with an MR compatible cryosurgical probe (Oncura SeedNet cryotherapy system). Images were acquired during

freezing, at echo times of 0.1, 0.4, 0.7, and 1.0 ms with the half pulse excitation, with and without the QP saturation bands. R2* maps were calculated from these images. The half pulse with the QP saturation pulse was also used in an *in vivo* canine prostate cryoablation to image frozen tissue around a cryoprobe. The animal study was conducted under protocol approved by the Stanford University Institutional Animal Care and Use Committee. A birdcage transmit coil, with receive-only endorectal coil was used in this study. The cryoprobes were placed through the anterior abdominal wall into the prostate. Imaging was performed in the coronal scan plane. R2* maps were obtained from images acquired at echo times of 0.2, 0.5, 0.8, and 1.1 ms during freezing.

Results

The suppression profile of the quadratic phase pulse compared to the default linear phase pulse is shown in Fig. 2. The higher bandwidth QP pulse achieves a much sharper profile than the default linear phase pulse. The transition width of the QP pulse is 2 mm, while the linear phase pulse transition width is approximately 1 cm.

Figure 3 plots the slice profile measurements of the half pulse, with and without the QP saturation RF pulse. In the presence of eddy currents, magnetization from outside the slice does not cancel properly, so the half RF pulse slice profile has tails that extend far beyond the desired slice. These tails are suppressed by the saturation bands, resulting in better slice selectivity.

The benefit of the improved excitation profile obtained with this method is illustrated in the following experiments. Figure 4 shows some short T2 vials imaged in the presence of out-of-slice long T2 signal, using the half RF with and without out-of-slice saturation. Figure 4a depicts the top view of the phantom setup. The imaged slice contained the short T2 vials (represented by the gray circles), and a long T2 sphere was placed adjacently out-of-slice. Due to poor slice selectivity resulting from eddy current errors, the half RF image in (b) shows significant out-of-slice signal contamination from the long T2 phantom (arrow). With the saturation bands, this out-of-slice signal is removed and a much better slice selection is achieved in (c). Figure 4d shows the streak artifacts that result without phase-cycling of the QP saturation pulse, while using the same gradient dephaser as in (c).

Figure 5 demonstrates the improvements in image quality and R2* quantitation achieved with improved slice localization. The phantom setup in (a) shows the slice imaged in the short T2 phantom, with a long T2 phantom placed out-of-slice. The line drawing shows T2* values measured in the short T2 phantom using non-slice-selective excitation to avoid eddy current errors. Without the saturation bands, there is signal from the out-of-slice long T2 phantom faintly visible in the magnitude image background (dashed arrow in (c)). The boundaries of some of the vials that are tilted also have artifacts (solid arrow). The grid lines in the middle of the phantom are blurred. These errors are also seen in the R2* maps (arrows). The saturation bands eliminate these artifacts by making the slice profile more selective. The magnitude images are also shown with a different contrast level in (d), so the out-of-slice signal is more noticeable. Even if the out-of-slice signal level is low, it induces errors in the R2* measurements of short T2 spins, as shown in Fig. 5(e) and Fig. 6. Figure 6 shows a comparison of the R2* values measured with and without the saturation bands. The R2* values measured by non-selective excitation lie along the identity line. The half pulse alone has errors, while measurements made with the half pulse plus the out-of-slice saturation bands are closer to the actual values.

Figure 7 and Figure 8 show the half pulse with out-of-slice saturation used to image frozen tissue. Figure 7 depicts the results of the *ex vivo* tissue freezing experiment. Without out-of-

slice saturation, the magnitude image shows signal artificially high at the position of the cryoprobe (arrow), and inside the iceball. The elevated R2* is an artifact of the time-varying eddy currents dephasing the signal. Both the magnitude and R2* images are improved with the saturation bands. Figure 8 shows magnitude images and R2* maps from an *in vivo* canine prostate cryoablation. Two cryoprobes inserted into the prostate were used to freeze tissue sequentially. The magnitude image shows the half pulse with the QP saturation bands used to image frozen tissue around one cryoprobe (with TE = 200 μs). The R2* map shows elevated R2* values in the frozen region. The cryoprobe artifact from the second probe without any frozen tissue, is seen as high R2* as well.

Discussion

UTE imaging with half pulse excitation is challenging as eddy current distortions of the gradient waveform cause errors in the half pulse slice profile and poor slice selectivity. Quantitation of short T2 signals has been elusive due to these problems. In most cases short T2 species are in the minority, and out-of-slice long T2 signal can overwhelm the short T2 signal within the desired slice when the slice profile is imperfect. This work demonstrates a simple and robust way to improve the half pulse profile by suppressing the out-of-slice signal to enhance slice localization. The wide and sharp quadratic phase saturation bands effectively suppress unwanted signal from outside the slice. Experimental results demonstrate substantially improved slice selectivity, and improved R2* quantitation. Thus, this approach can be useful in making short T2 imaging and quantitation less sensitive to eddy currents.

The profile of the saturation bands is very important for successful suppression of out-of-slice magnetization. Similar to other outer volume suppression applications, this requires pulses with a broad bandwidth, high selectivity and low errors in the remaining magnetization. An extremely sharp transition width is essential for successful out-of-slice suppression, as the bands being excited by the saturation pulse are closely spaced and are separated by just the slice thickness. The poor selectivity and transition profile of linear phase pulses limits their use in such cases. Quadratic phase (and other non-linear phase) pulses can achieve a large bandwidth and high selectivity, and so are very suitable for this application. Higher order polynomial phase pulses can potentially be used to achieve even higher bandwidths and/or shorter pulse durations in future work.

Like other saturation pulses, the suppression quality depends on the homogeneity of the applied RF. Errors in the flip angle, which can occur due to improper scaling of the RF amplitude on the scanner and spatial inhomogeneites in the RF transmit field, result in incomplete suppression of the outer volume signal. Large B_1 fluctuations can also distort the slice profile of the QP pulse, introducing ripples in the residual magnetization. Due to the high bandwidth of the QP saturation pulse, the edges of the saturation bands are not degraded by chemical shift errors. There is little effect of T1 relaxation on the suppression quality due to the relatively short pulse duration and gradient dephaser, before the half RF excitation.

A limitation of using spatial saturation to eliminate slice profile errors, is that it sacrifices the ability to do interleaved multi-slice imaging, in order to achieve good slice profile and selectivity. Nonetheless, the method is easy and robust to implement. This work was demonstrated on a 0.5T interventional scanner, but the results certainly apply to higher field strengths. At higher fields, RF power and SAR might be additional issues needing consideration. Combining the out-of-slice saturation with long T2 suppression within the slice of interest may also be useful to improve contrast for short T2 species, and to optimize the dynamic range for quantitation.

In summary, the out-of-slice saturation approach presented in this work provides a simple and reliable method that can be an effective alternative to the time-consuming gradient characterization and compensation techniques, and can be especially useful for quantitation of short T2s.

Acknowledgments

Funded by: NIH RO1 CA092061, P41 RR009784

References

1. Pauly, JM.; Conolly, SM.; Nishimura, DG.; Macovski, A. Slice-selective excitation for very short T2 species. Proceedings of SMRM; 1989. p. 28
2. Gatehouse PD, Bydder GM. Magnetic resonance imaging of short T2 components in tissues. Clinical Radiol. 2003; 58:1–19.
3. Robson MD, Gatehouse PD, Bydder M, Bydder GM. Magnetic resonance: an introduction to ultrashort TE imaging. J Comput Assist Tomogr. 2003; 27:825–846. [PubMed: 14600447]
4. Bergin CJ, Pauly JM, Macovski A. Lung parenchyma: projection reconstruction MR imaging. Radiology. 1991; 179:771–781. [PubMed: 2027990]
5. Gold GE, Pauly JM, Macovski A, Herfkens RJ. MR spectroscopic imaging of collagen: tendons and knee menisci. Magn Reson Med. 1995; 34:647–654. [PubMed: 8544684]
6. Robson MD, Bydder GM. Clinical ultrashort echo time imaging of bone and other connective tissues. NMR Biomed. 2006; 19:765–780. [PubMed: 17075960]
7. Reichert IL, Robson MD, Gatehouse PD, He T, Chappell KE, Holmes J, Girgis S, Bydder GM. Magnetic resonance imaging of cortical bone with ultrashort TE pulse sequences. Magn Reson Imaging. 2005; 23:611–618. [PubMed: 16051035]
8. Gold GE, Pauly JM, Glover GH, Moretto JC, Macovski A, Herfkens RJ. Characterization of atherosclerosis with a 1.5T imaging system. J Magn Reson Imaging. 1993; 3:399–407. [PubMed: 8448403]
9. Waldman A, Rees JH, Brock CS, Robson MD, Gatehouse PD, Bydder GM. MRI of the brain with ultrashort echo-time pulse sequences. Neuroradiology. 2003; 45:887–892. [PubMed: 14508620]
10. Nielsen HTC, Gold GE, Olcott EW, Pauly JM, Nishimura DG. Ultrashort echo time 2D time-of-flight MR angiography using a half pulse excitation. Magn Reson Med. 1999; 41:591–599. [PubMed: 10204884]
11. Butts K, Sinclair J, Daniel BL, Wansapura J, Pauly JM. Temperature quantitation and mapping of frozen tissue. J Magn Reson Imag. 2001; 13:99–104.
12. Balcom BJ, MacGregor RP, Beyea SD, Green DP, Armstrong RL, Bremner TW. Single point ramped imaging with T1 enhancement. J. Magn Reson. 1996; 123:31–34.
13. Idiyatullin D, Corum C, Park J, Garwood M. Fast and quiet MRI using a swept radiofrequency. J Magn Reson. 2006; 181:342–349. [PubMed: 16782371]
14. Rahmer J, Boernert P, Groen J, Bos C. Three dimensional radial ultrashort echo-time imaging with T2 adapted sampling. Magn Reson Med. 2006; 55:1075–1082. [PubMed: 16538604]
15. Brittain, J.; Shankaranarayanan, A.; Ramanan, V.; Shimakawa, A.; Cunnigham, C.; Hinks, S.; Francis, R.; Turner, R.; Johnson, J.; Nayak, K.; Tan, S.; Pauly, J.; Bydder, GM. Ultrashort TE imaging with single digit (8us) TE. Proceedings of ISMRM; 2004. p. 629
16. Wansapura JP, Daniel BL, Pauly JM, Butts K. Temperature mapping of frozen tissue using eddy current compensated half excitation RF pulses. Magn Reson Med. 2001; 46:985–992. [PubMed: 11675651]
17. Alley MT, Glover GH, Pelc NJ. Gradient characterization using a Fourier-transform technique. Magn Reson Med. 1998; 39:581–587. [PubMed: 9543420]
18. Duyn JH, Yang YH, Frank JA, Veen JW. Simple correction method for k-space trajectory deviations in MRI. J Magn Reson. 1998; 132:150–153. [PubMed: 9615415]

19. Gurney, P.; Pauly, J.; Nishimura, DG. A simple method for measuring B0 eddy currents. Proceedings of ISMRM; 2005. p. 866
20. Lu, A.; Daniel, BL.; Butts, K. A simple approach to measure and correct for B0 and linear eddy currents. Proceedings of ISMRM; 2006. p. 2378
21. Le Roux P, Gilles RJ, McKinnon GC, Carlier PG. Optimized outer volume suppression for single-shot fast spin-echo cardiac imaging. J Magn Reson Imaging. 1998; 8:1022–1032. [PubMed: 9786138]
22. Tran TKC, Vigneron DB, Sailasuta N, Tropp J, Le Roux P, Kurhanewicz J, Nelson S, Hurd R. Very selective suppression pulses for clinical MRSI studies of brain and prostate cancer. Magn Reson Med. 2000; 43:23–33. [PubMed: 10642728]
23. Luo Y, De Graaf RA, DelaBarre L, Tannus A, Garwood M. BISTRO: An outer volume suppression method that tolerates RF field inhomogeneity. Magn Reson Med. 2001; 45:1095–1102. [PubMed: 11378888]
24. Kunz DW. Use of frequency modulated radio frequency pulses in MR imaging experiments. Magn Reson Med. 1986; 3:377–384. [PubMed: 3724417]
25. Schulte RF, Tsao J, Boesiger P, Pruessmann KP. Equi-ripple design of quadratic phase RF pulses. J Magn Reson. 2004; 166:111–122. [PubMed: 14675826]
26. Schulte RF, Hennig A, Tsao J, Boesiger P, Pruessmann KP. Design of broadband RF pulses with polynomial phase response. J Magn Reson. 2007; 186:167–175. [PubMed: 17331765]
27. Shinnar, M. Selective excitation pulses requiring less peak power. Proceedings of SMR; 1994. p. 122
28. Pauly JM, Le Roux P, Nishimura DG, Macovski A. Parameter relations for the Shinnar-Le Roux selective excitation pulse design algorithm. IEEE T Med Imaging. 1991; 10:53–65.
29. Zur Y, Wood ML, Neuringer LJ. Spoiling of transverse magnetization in steady-state sequences. Magn Reson Med. 1991; 21:251–263. [PubMed: 1745124]

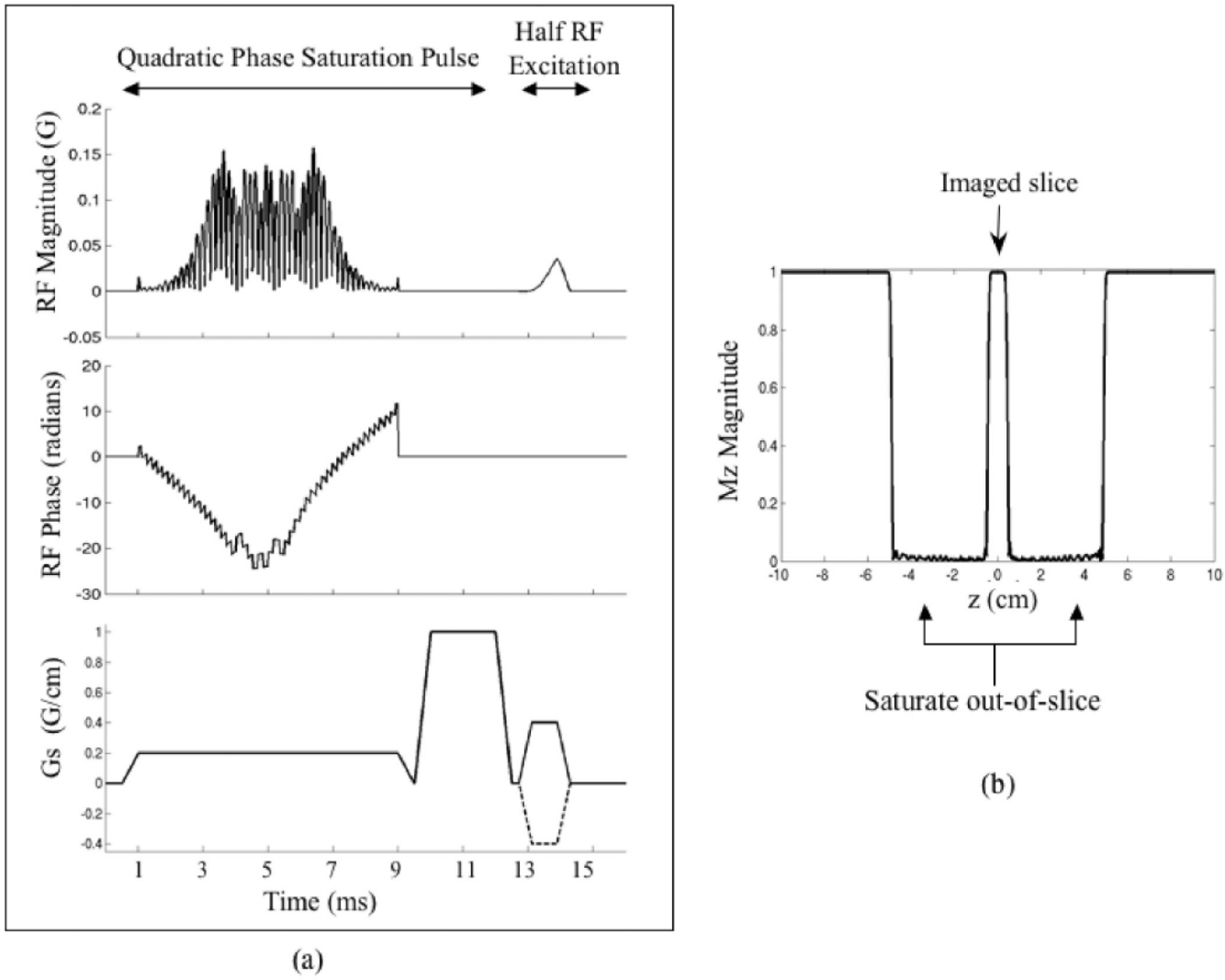

Figure 1.

(a) Pulse diagram of the RF excitation part of the 2D UTE sequence. The QP spatial saturation RF and dephaser is followed by half RF excitation. A 2nd excitation with inverted slice-select gradient (dotted line) is used to convert the half pulse into a full pulse. (b) The simulated slice profile for the cosine modulated quadratic phase RF pulse. It achieves saturation bands 4.5 cm wide with a transition width of 2 mm, on each side of the imaged slice.

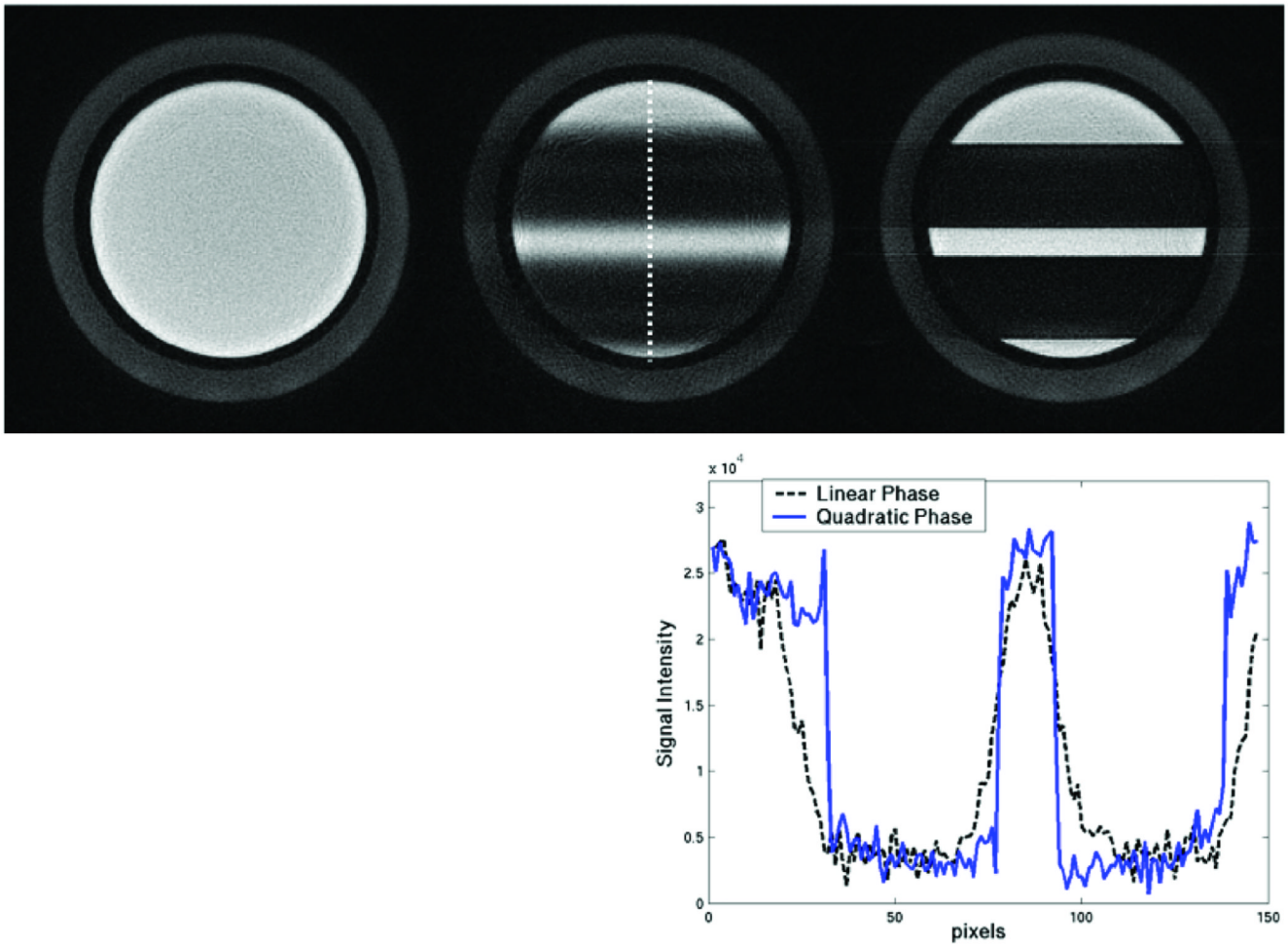

Figure 2.
Comparison of the saturation profile of the default linear phase pulse profile (middle) versus the QP pulse (right). The left image is without any saturation bands, for reference. The intensity profile of the saturation bands along the dotted line is shown in the plot. The QP pulse has 4 times the bandwidth of the linear phase pulse, and so its saturation bands are much sharper than the linear phase sat bands.

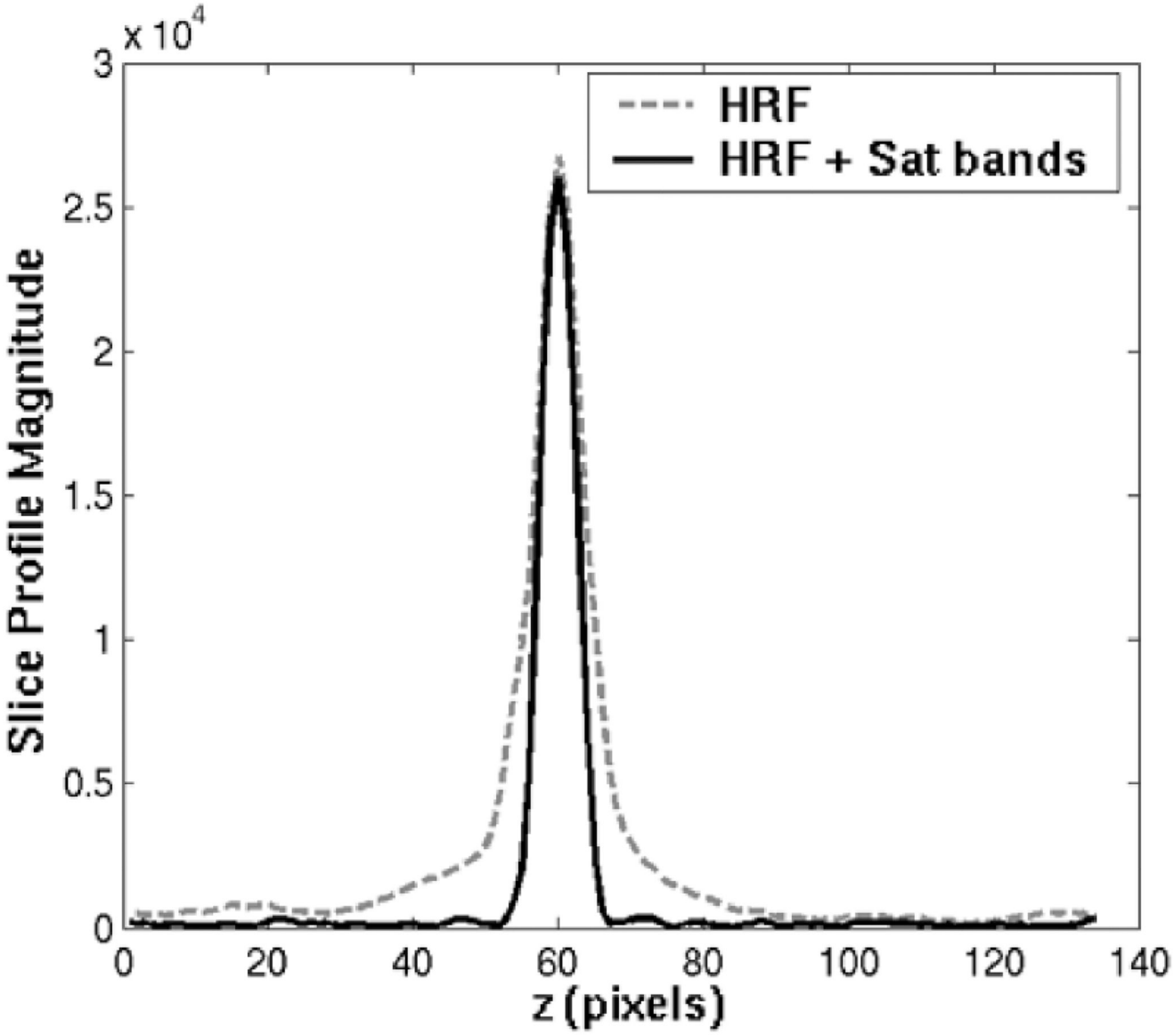

Figure 3.
The slice profile magnitude measured with half RF with (solid line) & without (dashed line) QP saturation in the slice direction. The phantom T2 was 100 ms and the TE was 100 μs. The out-of-slice saturation bands greatly improve the slice selectivity.

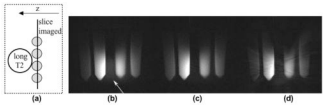

Figure 4.

Comparison of images with short T2 (1–20 ms) vials imaged with a TE of 200 μs. (a) Top view of the phantom setup shows the imaged slice containing short T2 vials (represented by the gray circles), with a long T2 sphere placed out-of-slice. With no out-of-slice saturation (b), the image demonstrates out-of-slice signal (arrow). With QP saturation (c), the out-of-slice signal is eliminated. Figure (d) demonstrates a streak artifact that resulted when the QP saturation pulse was not phase-cycled, with the same gradient dephaser as in (c).

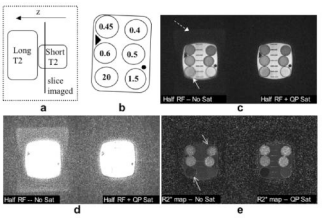

Figure 5.

A short T2 phantom was imaged with a long T2 phantom placed adjacently, but out-of-slice, as shown in the phantom setup (a). The line diagram shows the T2* (ms) values in the phantom (b). Without the saturation bands in (c) - left, there is signal from the out-of-slice long T2 phantom faintly visible in the background of the magnitude image (dashed arrow). The boundaries of some of the vials that are tilted also have artifacts (solid arrows). The grid lines in the middle of the phantom are blurred. The saturation bands eliminate these artifacts by making the slice profile more selective. With a different contrast-level of the magnitude image (d), the out of slice signal is more visible. Even if the out-of-slice signal level is low, it induces errors in the R2* measurements of the short T2 spins. The corresponding R2* maps (e) also show improvement with the sat bands.

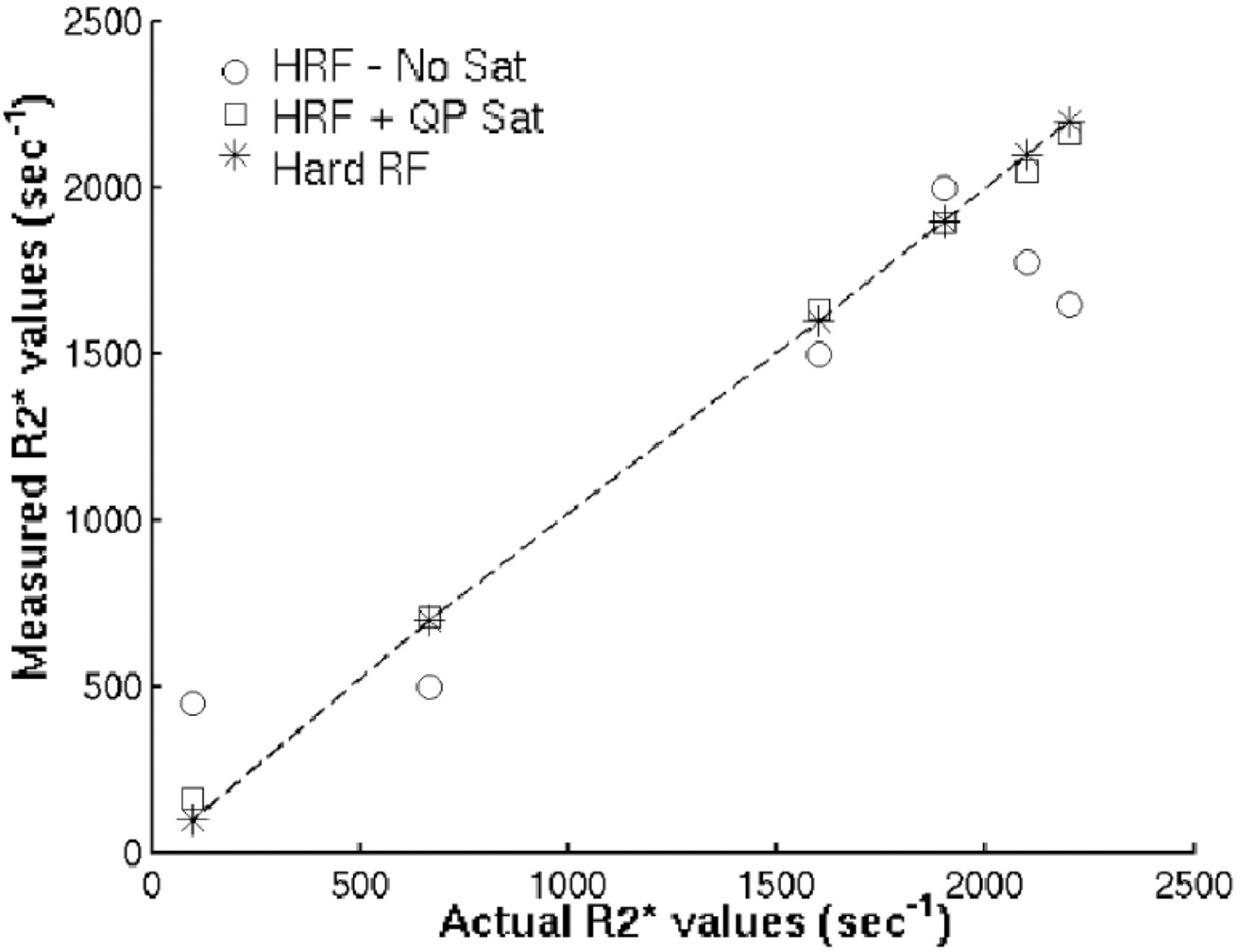

Figure 6.
Actual *vs*. measured R2* values, for the images in Fig. 5. Actual R2* values, measured with non-selective hard RF excitation, lie along the identity line (*). Each column is a different vial. Half RF (HRF) measurements have obvious errors, while Half RF + Sat band measurements are closer to the actual values.

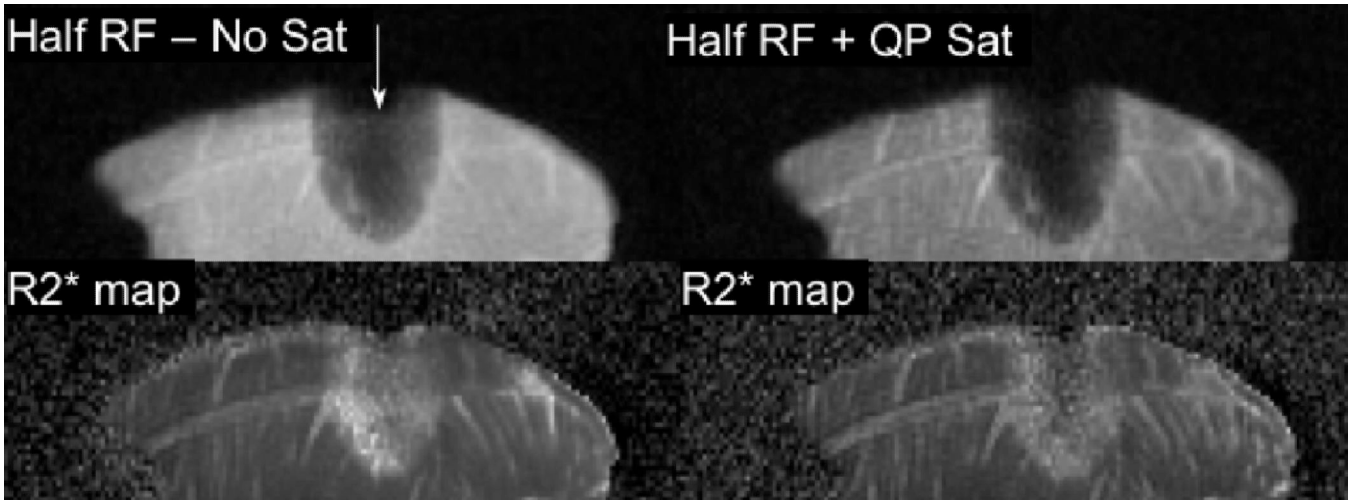

Figure 7.
Magnitude (top row) and R2* (bottom row) images of *ex vivo* frozen tissue, using half RF excitation without & with out-of-slice saturation (TE =100 μs). Arrow shows location and orientation of cryoprobe. Without the saturation bands, there is significant out-of-slice signal contribution adding into the desired slice within the iceball, leading to artificially high R2* measurements. There is high signal intensity and blurring in the unfrozen tissue due to poor slice selectivity. Both magnitude and R2* images are dramatically improved with the saturation bands.

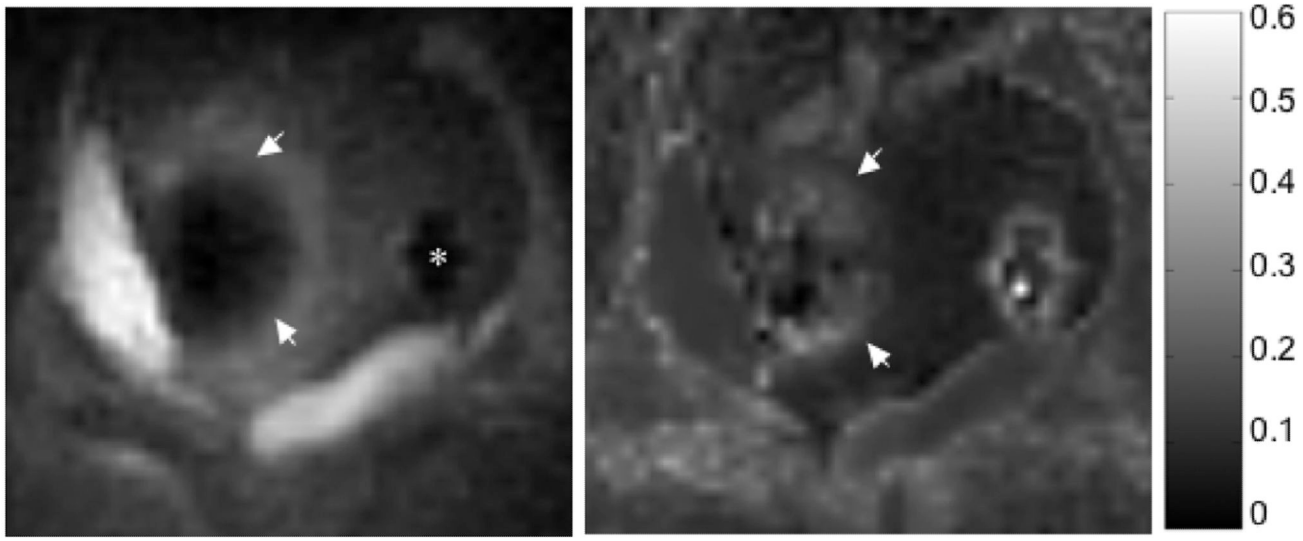

Figure 8.

In vivo canine prostate cryoablation - magnitude (left) and R2* map (right) of frozen tissue. Two cryoprobes were inserted into the prostate. The magnitude image shows frozen tissue around 1 cryoprobe (arrows), imaged with the half pulse with QP saturation at TE=200 μs. R2* values were calculated from images at TE = 0.2, 0.5, 0.8, 1.1 ms, and are elevated in the frozen tissue. The colorbar on the right shows the scale of the R2* values in ms^{-1}. The * marks the cryoprobe artifact from the 2nd probe without any frozen tissue, and is seen as high R2* as well.